PIER Letters

(Received 13 May 2024, Accepted 3 July 2024, Scheduled 6 July 2024)

Design and Performance of a Fully-Polarized Tightly-Coupled Patch Antenna for Advanced Phased Array Radar Systems

Jianjun Wu*, Zhao Li, and Hongbing Sun

Nanjing Research Institute of Electronics Technology, Nanjing 210039, China

ABSTRACT: A tightly-coupled patch array antenna, capable of broadband operation and low profile, is proposed in this study. The antenna subarray comprises four closely-coupled square patches that rotate in sequence. An impedance matching strip is utilized to achieve broadband matching of the antenna. By configuring the subarray with various feeding phases, it is possible to achieve the switching of six polarization states. The simulated and measured results suggest that the proposed antenna demonstrates a broad impedance matching band ranging from 4.2 GHz to 5.25 GHz (22.2%) over a scanning angle span of $\pm 45^\circ$, while maintaining a low profile of $0.033\lambda_0$. The antenna's inherent simple structure, low profile, wide bandwidth, and favorable radiation characteristics position it as a promising option for multi-function phased array radar systems.

1. INTRODUCTION

The development of radar polarization theory and technology has rendered polarization an essential technical tool for contemporary intelligent radar systems. The utilization of target polarization measurement technology enables the acquisition of more comprehensive and detailed information regarding the target. This, in turn, enhances the probability of accurately recognizing radar targets [1]. The incorporation of fully-polarized phased array radar with precise polarization measurement capability represents a significant advancement of future multifunctional phased array radar systems, particularly in the fields of weather observation and aircraft identification [2]. A fully polarized phased array antenna is commonly designed using two orthogonal polarization modes [3]. Each polarization channel is linked to transmit/receive (T/R) modules to achieve beam scanning, flexible control of beam shaping, and rapid switching of polarization states [4]. For fully-polarized phased array antennas, antenna designers aim to significantly reduce cross-polarization levels [5], while ensuring minimal variation in the antenna's polarization characteristics during broadband wide-angle scanning [6].

Patch antennas offer benefits such as being lightweight, having a low profile, and being easily adaptable, making them extensively utilized in diverse wireless systems [7]. Patch antennas can readily achieve multiple polarization radiations. Due to the relatively narrow bandwidth of patch antennas and the significant coupling between patch array elements, and the most of research on patch antennas focuses on broadening the bandwidth [8] and suppressing coupling [9]. In the past decade, numerous ultra-wideband arrays utilizing tight coupling effects have been suggested, encompassing both linearly polarized and dual-polarized antenna arrays. The predominant antenna configurations characterized by tight coupling include dipole [10] and octagonal ring [11]. Irci et al. introduced a novel patch antenna design leveraging the tight coupling effect. This innovation led to an enhancement in the bandwidth of conventional patch antennas from 2.5% to 5.6% [12] and 17.3% [13]. The results indicate that the interconnection of patch antennas can enhance the bandwidth of the patch antenna while preserving its low-profile advantages. Following this, several patch antenna designs leveraging tight coupling effects have been consistently investigated. These designs include interconnected patch arrays [14], patches with U-shaped slots that exhibit tight coupling [15], and coupling patches for circular polarization [16, 17].

Additionally, a patch antenna with multiple feeding points is suggested as a means to attain fully polarized radiation [18]. In [19] by Wu et al., a single patch is fed by four aperture-coupled slots, enabling the provision of four polarization states. In [20, 21] by Duan et al., it is possible to achieve six polarization states by conveniently adjusting the input phases of the four ports in the patch antenna. Four substrate integrated waveguide (SIW) cavity-backed cross-slot antennas are created through the process of etching two orthogonal slots on a square patch [22]. Dual circular polarizations can be achieved through the utilization of an additional six-port feeding network. The multiple-feeding method offers convenience for the design of fully polarized antennas.

In this study, a fully-polarized tightly coupled patch antenna array is introduced. The study examines the effect of the coupling between patch elements on the broadening of antenna bandwidth. The 4-element subarray can be conceptualized as four closely interconnected patches with four feeding points. Six polarization states can be readily altered by adjusting the feeding phase of the T/R modules within the phased array. Favorable impedance matching and polarization performance can be maintained even when the beam is scanned at angles up

* Corresponding author: Jianjun Wu (wujj2024@126.com).

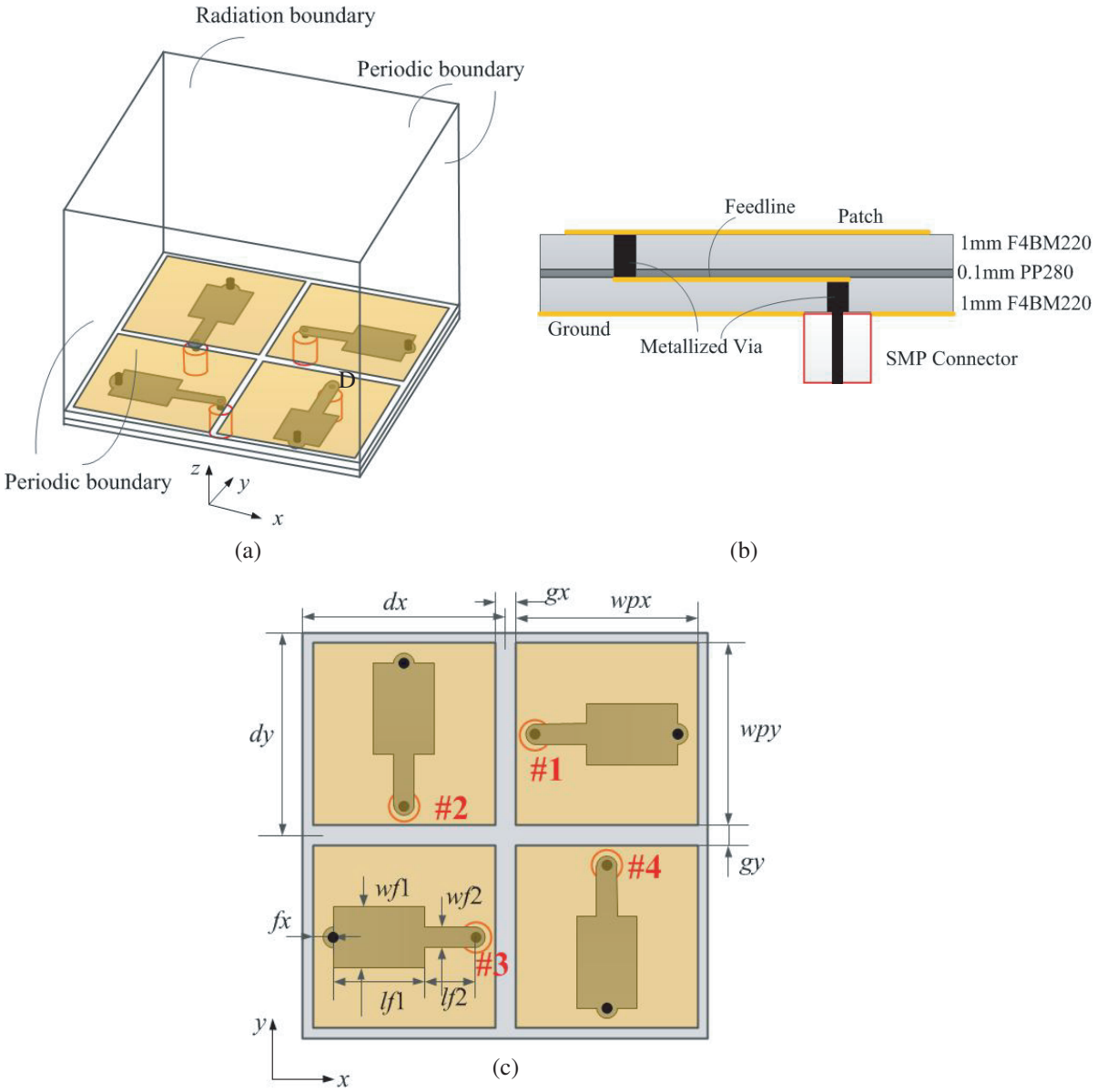

FIGURE 1. Geometries of tightly-coupled patch antenna subarray: (a) 3-D view; (b) Side view; (c) Top view. (Dimensions: $dx = dy = 16\,\text{mm}$, $gx = gy = 1\,\text{mm}$, $wpx = wpy = 15\,\text{mm}$, $wf1 = 5\,\text{mm}$, $lf1 = 6.25\,\text{mm}$, $wf2 = 1.5\,\text{mm}$, $lf2 = 5\,\text{mm}$, $fx = 2.5\,\text{mm}$).

to $\pm 45°$. The proposed tightly coupled patch antenna shows promise as a suitable option for multifunction phased array radar antennas.

2. ANTENNA DESIGN AND OPERATIONAL PRINCIPLES

2.1. Structure of 2 × 2 Subarray

The geometry of the proposed closely integrated patch antenna subarray is illustrated in Figure 1. The antenna subarray consists of four identical patch elements that exhibit rotational symmetry along the center of the subarray. The spacing between the patch elements is $0.25\lambda_0$, where λ_0 represents the wavelength in free space corresponding to the center operating frequency of 4.75 GHz. In the simulation model, the subarray boundary is defined as a periodic boundary. The antenna subarray has the potential for additional expansion into a two-dimensional array in both the x and y directions.

In Figure 1(b), the antenna under consideration comprises two layers of F4B substrates, each 1 mm thick (with relative permittivity $\varepsilon_r = 2.2$ and loss tangent $\tan\delta = 0.0009$), sandwiching a layer of PP28, 0.1 mm thick (with relative permittivity $\varepsilon_r = 2.8$ and loss tangent $\tan\delta = 0.001$). The overall thickness of the antenna is 2.1 mm, representing merely $0.033\lambda_0$. In addition to connecting the upper and lower F4B boards, PP28 is used as a medium layer. Since the antenna profile is very small, the influence of the 0.1 mm PP28 cannot be ignored and should be included in the simulation model. The square patch is situated on the topmost layer of the upper substrate. The lower

TABLE 1. Phase configuration of different polarization states.

Port	0°-LP	90°-LP	LHCP	RHCP	+45°-LP	-45°-LP
#1	0°	Load	0°	270°	0°	0°
#2	Load	0°	90°	180°	0°	180°
#3	180°	Load	180°	90°	180°	180°
#4	Load	180°	270°	0°	180°	0°

substrate's underside serves as the grounding for the antenna. The antenna ground is welded to sub miniature push-on (SMP) connector for the purpose of feeding. To achieve broadband impedance matching, a feeding strip-line with varying widths is inserted between the two substrates. The two terminals of the feeding strip-line are linked to the upper patch and the inner conductor of SMP connector via metallized vias with a diameter of 0.5 mm.

Figure 2 depicts the isolation among the four elements within the antenna subarray. The strong coupling (approximately -5 dB) between ports 1 and 3 is evident, attributed to the similar polarization of radiation. Given that port 1 and ports 2/4 are situated at the orthogonal polarized feeding point, the interaction between port 1 and ports 2/4 exhibits weak coupling, measuring below -15 dB.

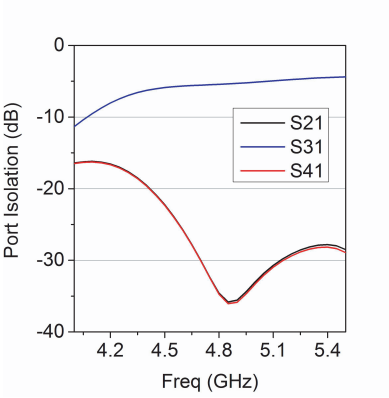

FIGURE 2. Simulated isolation between port 1 and ports 2/3/4.

2.2. Phase Configuration of Different Polarization States

Table 1 outlines the phase configurations of the four ports within the antenna subarray to establish various polarization states. When ports 1/3 are stimulated with a phase difference of 180° and ports 2/4 terminated with a load, 0° linear polarization (0°-LP) is established. When ports 2/4 are stimulated, with a phase difference of 180° and ports 1/3 is terminated with a load, 90° linear polarization (90°-LP) is generated. When ports 1–4 are excited simultaneously with a phase difference of 90°, they generate either right-hand circular polarization (RHCP) or left-hand circular polarization (LHCP). When ports 1–4 are excited simultaneously with a phase difference of 0/180°, ±45° polarization (±45°-LP) is achieved.

It is important to note that the feeding amplitude remains constant in the aforementioned phase configuration. Furthermore, alternative linear polarization angles can be generated by adjusting the port amplitude. In an active phased array system, the amplitude and phase of the antenna ports can be rapidly configured and switched using T/R modules. Therefore, the feeding network is removed in our design because the antenna is directly connected to chipped T/R modules.

Figure 3 presents the current distribution on the patch surface of the antenna under 0°-LP, 90°-LP, and RHCP polarization states. Taking 0°-LP as an example, when port 1 and port 3 are excited, x-direction currents are induced in patches 1 and 3. Patches 2 and 4 can be considered as parasitic patches, which also couple x-direction currents. In RHCP configuration, the current direction on the four patches undergoes rotation over time.

2.3. Impedance Matching Feeding Strip

Figure 4 illustrates a comparison of voltage standing wave ratio (VSWR) among four different types of patch antennas. Antenna I is a patch antenna that is fed directly by the probe, exhibiting a bandwidth of only 7.6% (4.56–4.92 GHz). Antenna II is characterized by a single antenna design integrated with an impedance-matching feeding line. The bandwidth has been expanded, but the impedance is poorly matched. Antenna III is a patch antenna that is tightly coupled and directly fed by the probe, exhibiting a minimum VSWR of 2. Antenna IV, on the other hand, is a proposed tightly coupled antenna that incorporates impedance matching in its feeding line. The impedance bandwidth of the system spans 22.2% (4.2–5.25 GHz) for VSWR values below 1.8. The quality factor of the antenna is lowered by the coupling between the adjacent patches, which corresponds to wider bandwidth. In Antenna IV, the feeding probe is equivalent to inductance. The capacitive component between the feeding strip and the patch/ground can offset the inductance. Therefore, better impedance matching can be obtained in Antenna IV.

2.4. Phase Configuration for Scanning Array

When expanding the subarray into an antenna array, two strategies can be employed to configure the phase of the subarray during the scanning of the array beam (Figure 5). Taking LHCP scanning in the XOZ-plane as an example, strategy 1 involves adding the scanning phase difference φ_x to each unit respectively. Strategy 2 considers the four-element subarray as a unified entity, where the phase difference between subarrays is

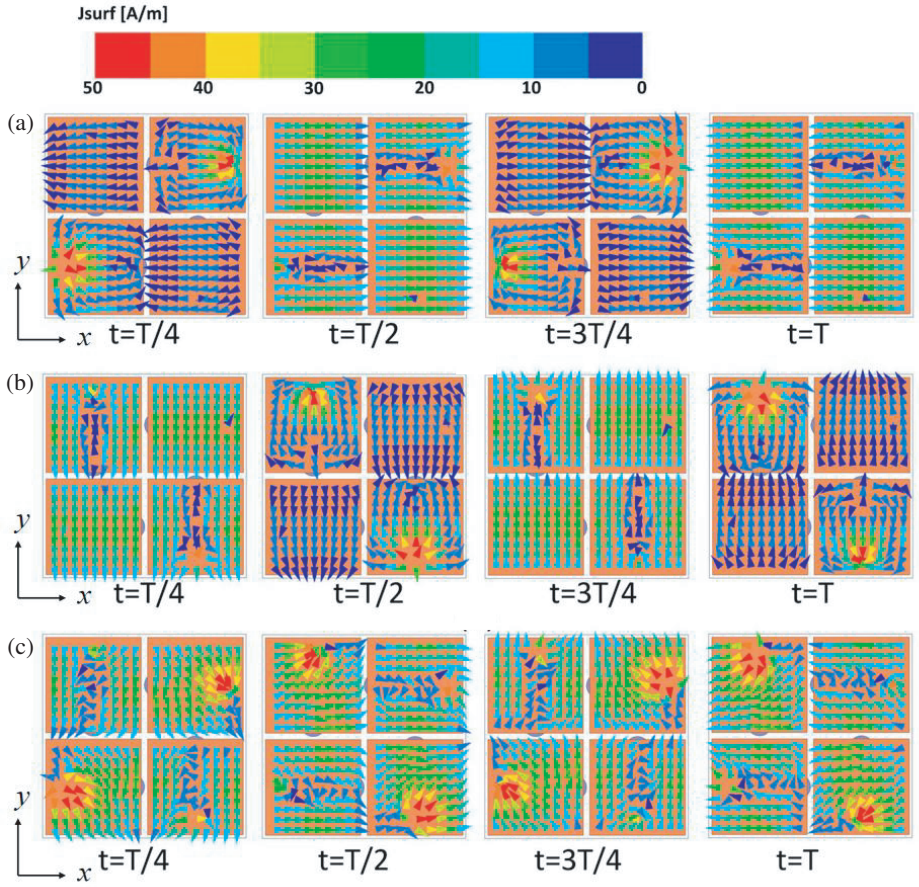

FIGURE 3. Current distributions in patch antenna subarray for different polarization states: (a) 0°-LP; (b) 90°-LP; (c) RHCP.

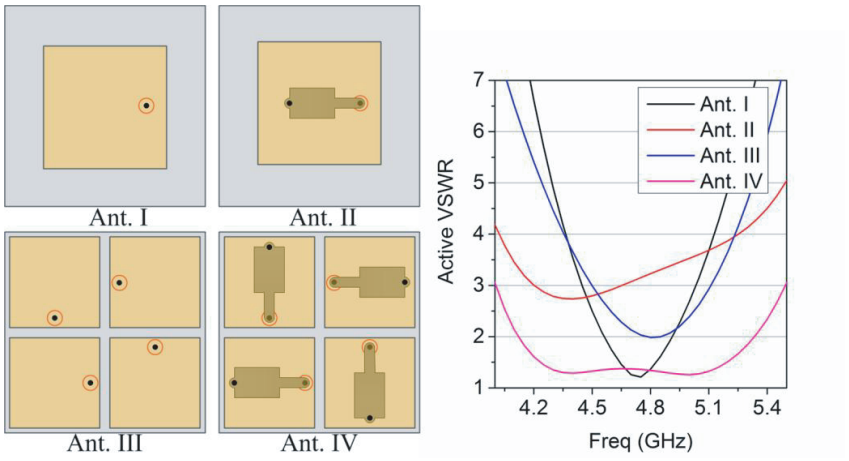

FIGURE 4. Schematic and active VSWR of four patch antenna designs.

$2\varphi_x$, which can be determined as follows:

$$\varphi_x = kd_x \sin\theta$$

where θ is the beam scanning angle. The active VSWR of the two-phase configuration methods is depicted in Figure 6. The analysis reveals that the phase gradient of the antenna is significant in strategy 2, leading to poor impedance matching during large-angle scanning. Strategy 1 exhibits a reduced phase gradient attributed to the shorter distance between elements, resulting in improved impedance matching performance.

3. PROTOTYPE AND RESULTS

Figure 7 shows the images of the constructed prototype of an antenna array, comprising 7 × 7 subarrays, totaling 196 antenna elements. The antenna array utilizes printed circuit board

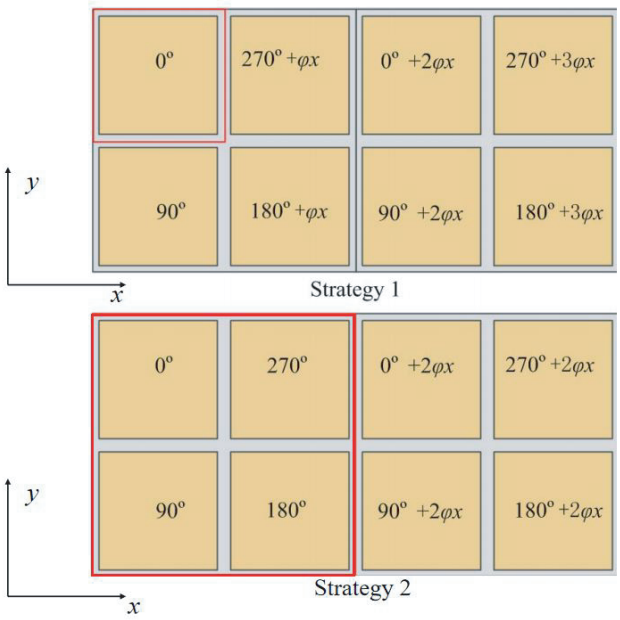

FIGURE 5. Schematic of two phase configuration strategies for scanning arrays.

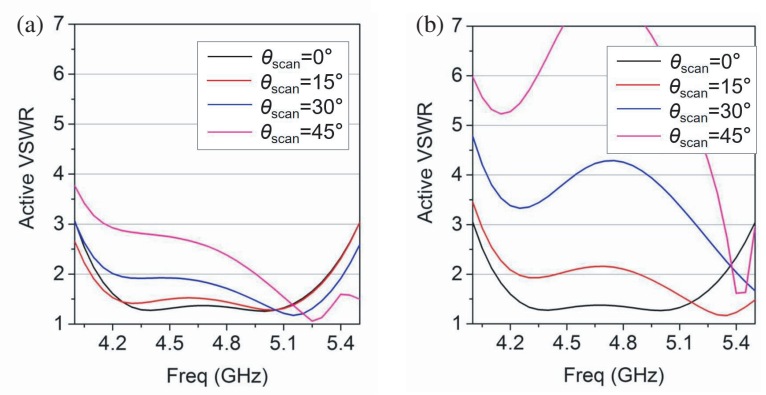

FIGURE 6. Active VSWR of port 1 for RHCP state during scanning from 0° to 45° in XOZ-plane under phase configuration methods: (a) Method 1 and (b) Method 2.

(PCB) processing technology, with SMP connectors soldered onto the back of the antenna for testing purposes. The testing method in the proposed paper can quickly evaluate the array performance under different polarization states.

The method used for measuring the active VSWR of the antenna array is based on the approach outlined in [23] by Kalfa and Halavut. Firstly, the self-reflection coefficient of the central element and the coupling coefficient between the central element and all other units are assessed. The active S parameters are then computed, taking into account the coupling between elements and the scanning phase for various polarization states. The simulation and measurement of the active VSWR are depicted in Figure 8. The antenna exhibits a bandwidth of 22.2% (4.2–5.25 GHz) with a VSWR less than 1.8 in the broadside direction. When the array is scanned at 45°, the active VSWR is below 3. Figure 9 illustrates VSWR of the array scanning at a 45° angle on a two-dimensional plane. The two-dimensional active VSWR remains below 2 for the majority of angles. Due to the advanced PCB processing technology, each antenna channel has very high consistency. Testing the performance of one or a few units can reflect the performance of the entire antenna array. It is noteworthy that the active VSWR test results of neighboring elements to this particular element exhibit similarities to the results presented in Figure 8, necessitating solely a rotation in the relevant coordinate direction.

The array's radiation performance is evaluated in a microwave anechoic chamber. The method of active element pattern testing described in [24] by Pozar involves feeding only the central element while connecting the other elements to the matching load. The scanning pattern of the antenna array is determined by multiplying the active pattern of the central element by the scanning antenna array factor. When the scale of the antenna array is large enough, the method of active element pattern testing is approximately identical to evaluate the

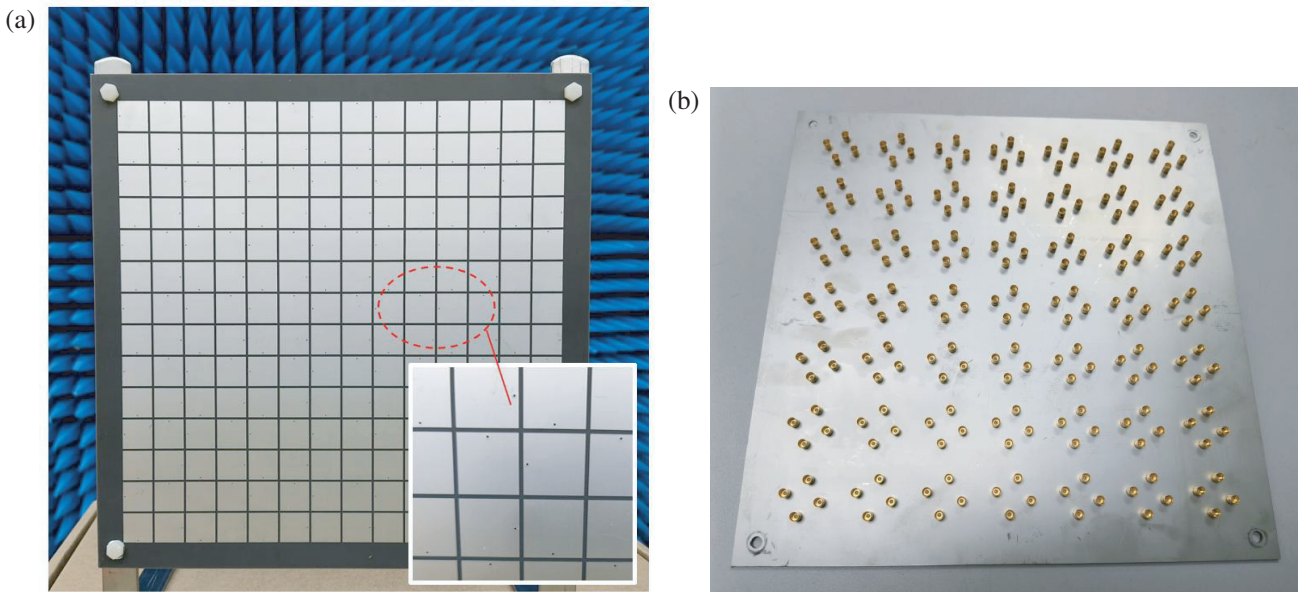

FIGURE 7. Photographs of fabricated prototype: (a) Top view and (b) Bottom view.

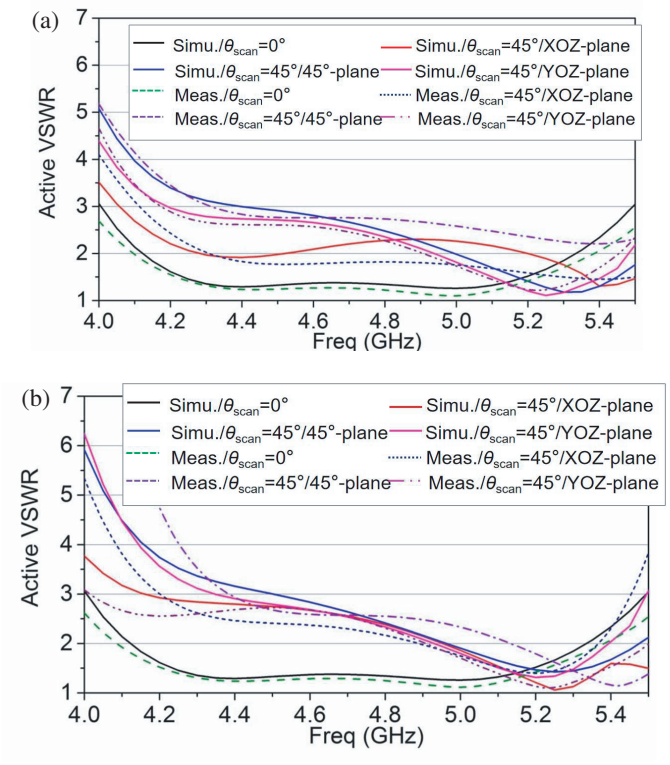

FIGURE 8. Simulated and measured active VSWRs: (a) 0°-LP and (b) LHCP states.

scanning performance of the antenna array. Figure 10 illustrates the co-polarization and cross-polarization characteristics of the central antenna element in three standard planes. The wide beamwidth of the antenna indicates the scanning capability of the antenna array. The calculated scanning pattern of the antenna array is depicted in Figure 11. The decrease in scanning gain is below 3 dB at a scanning angle of 45°. The cross-polarization is below −25 dB, indicating a lower level than the cross-polarization present in the active element pattern. The cross-polarization is mitigated by the 180° phase shift between ports 1/3 and ports 2/4.

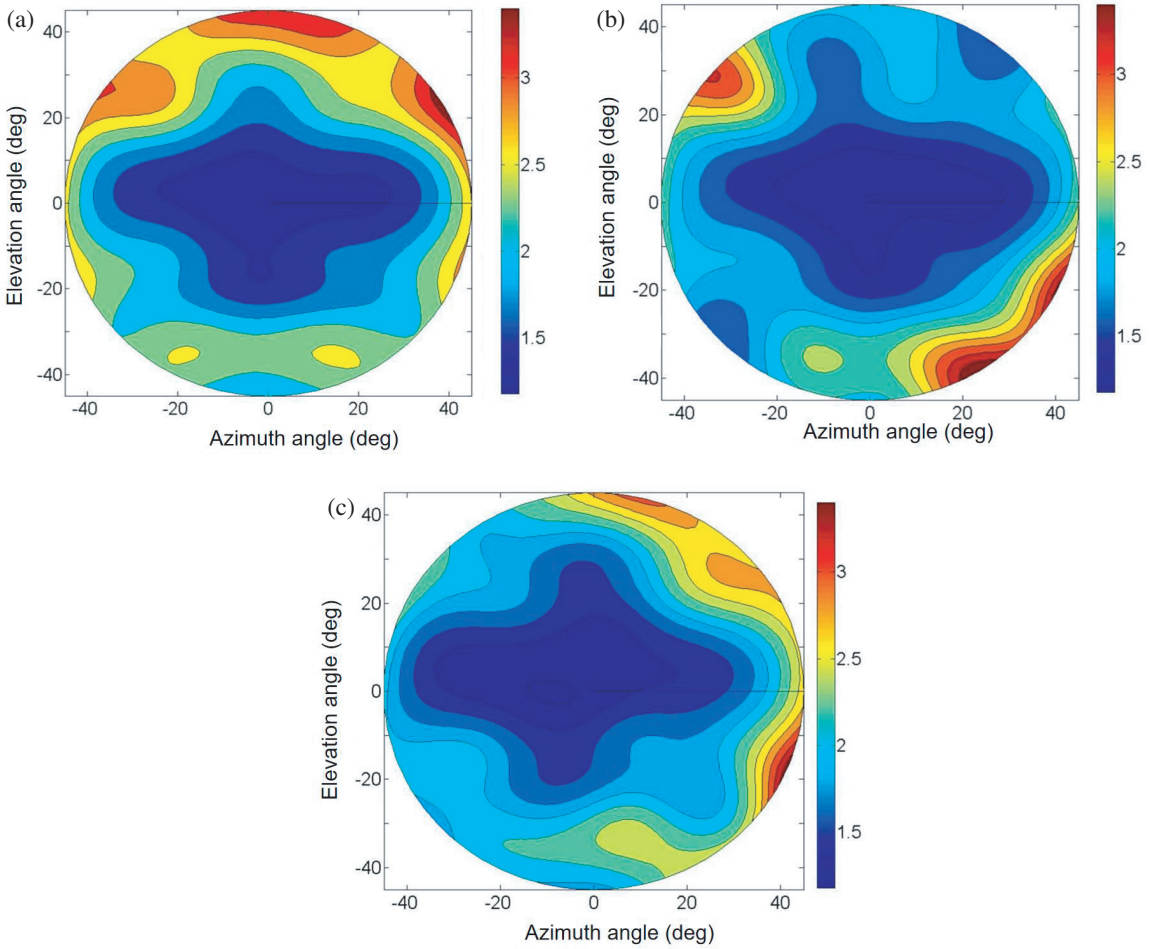

FIGURE 9. Active VSWR of port 1 at 4.75 GHz for various polarization states during scanning from 0° to 45° in 2D plane: (a) 0°-LP; (b) 45°-LP; (c) LHCP.

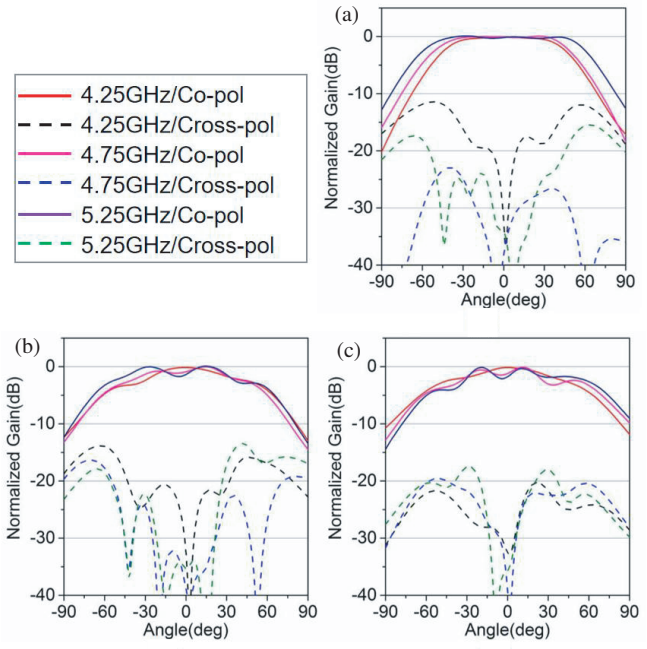

FIGURE 10. Measured active element pattern of patch 1 in various planes: (a) xoz-plane; (b) $+45°$-plane; (c) yoz-plane.

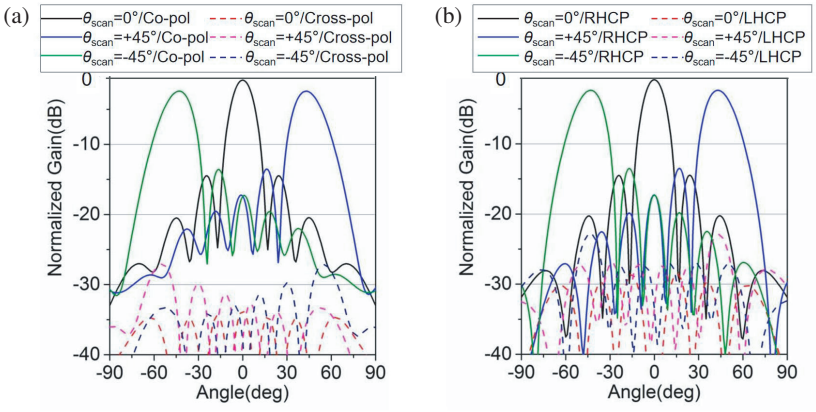

FIGURE 11. Calculated normalized patterns at 4.75 GHz in xoz-plane for various states: (a) 0°-LP state and (b) RHCP state.

4. CONCLUSION

A novel broadband fully-polarized patch antenna utilizing the tight-coupling effect is introduced in this study. Through the utilization of close arrangement of antenna element, rotating patch placement and broadband impedance matching technology, the antenna has attained an impedance bandwidth of 22.2% while maintaining a low profile of $0.033\lambda_0$. Through various phase configurations, the antenna can readily attain different polarization states, including 0°-LP, 90°-LP, circular polarization, and oblique polarization. The antenna suggested in this article represents a viable option for a multifunctional phased array radar system.

REFERENCES

[1] Palmer, R. D., M. B. Yeary, D. Schvartzman, J. L. Salazar-Cerreno, C. Fulton, M. McCord, B. Cheong, D. Bodine, P. Kirstetter, H. H. Sigmarsson, *et al.*, "Horus — A fully digital polarimetric phased array radar for next-generation weather observations," *IEEE Transactions on Radar Systems*, Vol. 1, 96–117, 2023.

[2] Stailey, J. E. and K. D. Hondl, "Multifunction phased array radar for aircraft and weather surveillance," *Proceedings of the IEEE*, Vol. 104, No. 3, 649–659, 2016.

[3] Wang, Y., J. Zhou, Z. Wang, C. Pang, Y. Li, and X. Wang, "Low-cost architecture using interleaved thinning for polarimetric phased array," *IEEE Antennas and Wireless Propagation Letters*, Vol. 23, No. 3, 980–984, 2023.

[4] Fulton, C. and W. Chappell, "Calibration of panelized polarimetric phased array radar antennas: A case study," in *2010 IEEE International Symposium on Phased Array Systems and Technology*, 860–867, Waltham, MA, USA, 2010.

[5] Pang, C., J. Dong, T. Wang, and X. Wang, "A polarimetric calibration error model for dual-polarized antenna element patterns," *IEEE Antennas and Wireless Propagation Letters*, Vol. 15, 782–785, 2015.

[6] Dai, H., X. Wang, J. Luo, Y. Li, and S. Xiao, "A new polarimetric method by using spatial polarization characteristics of scanning antenna," *IEEE Transactions on Antennas and Propagation*, Vol. 60, No. 3, 1653–1656, 2012.

[7] Zhou, E., Y. Cheng, F. Chen, H. Luo, and X. Li, "Low-profile high-gain wideband multi-resonance microstrip-fed slot antenna with anisotropic metasurface," *Progress In Electromagnetics Research*, Vol. 175, 91–104, 2022.

[8] Tran, H. H. and N. Nguyen-Trong, "Performance enhancement of MIMO patch antenna using parasitic elements," *IEEE Access*, Vol. 9, 30 011–30 016, 2021.

[9] Qian, J.-F., S. Gao, B. Sanz-Izquierdo, H. Wang, H. Zhou, and H. Xu, "Mutual coupling suppression between two closely placed patch antennas using higher-order modes," *IEEE Transactions on Antennas and Propagation*, Vol. 71, No. 6, 4686–4694, 2023.

[10] Zhou, Y., F. Zhu, S. Gao, Q. Luo, L.-H. Wen, Q. Wang, X. Yang, Y. Geng, and Z. Cheng, "Tightly coupled array antennas for ultra-wideband wireless systems," *IEEE Access*, Vol. 6, 61 851–61 866, 2018.

[11] Chen, Y., S. Yang, and Z.-P. Nie, "A novel wideband antenna array with tightly coupled octagonal ring elements," *Progress In Electromagnetics Research*, Vol. 124, 55–70, 2012.

[12] Irci, E., K. Sertel, and J. L. Volakis, "An extremely low profile, compact, and broadband tightly coupled patch array," *Radio Science*, Vol. 47, No. 03, 1–13, 2012.

[13] Irci, E., K. Sertel, and J. L. Volakis, "Bandwidth enhancement of low-profile microstrip antennas using tightly coupled patch arrays," in *2011 IEEE International Symposium on Antennas and Propagation (APSURSI)*, 1044–1047, Spokane, WA, USA, 2011.

[14] Yang, X., P.-Y. Qin, Y. Liu, Y.-Z. Yin, and Y. J. Guo, "Analysis and design of a broadband multifeed tightly coupled patch array antenna," *IEEE Antennas and Wireless Propagation Letters*, Vol. 17, No. 2, 217–220, 2017.

[15] Li, D., B. Yu, W. Li, X. Zhu, and X. Yuan, "Broadband integrated differentially-fed patch antenna with tightly-coupled elements," *IEEE Antennas and Wireless Propagation Letters*, Vol. 22, No. 10, 2457–2461, 2023.

[16] Son, D.-C., A. Samaiyar, M. A. Elmansouri, and D. S. Filipovic, "Design of a circularly-polarized tightly-coupled microstrip patch array," in *2021 IEEE International Symposium on Antennas and Propagation and USNC-URSI Radio Science Meeting (APS/URSI)*, 513–514, Singapore, 2022.

[17] Xie, X., L. Zhang, M. Wang, W. Li, C. Mao, and Y. He, "Circularly polarized tightly coupled quarter-circle truncated patch array," in *2022 International Applied Computational Electromagnetics Society Symposium (ACES-China)*, 1–3, Xuzhou, China, 2022.

[18] Liu, N.-W., J.-L. Fan, L. Zhu, Q. Wu, Y. Liu, and S. Sun, "Mutual-coupling reduction of a quad-port cross-slot antenna with simultaneously co-polarized and dual-polarized patterns," *IEEE Transactions on Antennas and Propagation*, Vol. 72, No. 2, 1140–1149, 2024.

[19] Wu, Y.-F., C.-H. Wu, D.-Y. Lai, and F.-C. Chen, "A reconfigurable quadri-polarization diversity aperture-coupled patch antenna," *IEEE Transactions on Antennas and Propagation*, Vol. 55, No. 3, 1009–1012, 2007.

[20] Duan, W., S. Liao, X. Y. Zhang, Y. C. Li, and Q. Xue, "Multi-port patch antennas for flexible power combining and feeding choice," *IEEE Access*, Vol. 6, 79 094–79 104, 2018.

[21] Duan, W., X. Y. Zhang, S. Liao, K. X. Wang, and Q. Xue, "Multiport power combining patch antenna with stable reflection coefficient and radiation pattern in six polarization states," *IEEE Transactions on Antennas and Propagation*, Vol. 67, No. 2, 719–729, 2019.

[22] Yan, Y.-D., Y.-C. Jiao, H.-T. Cheng, and C. Zhang, "A low-profile dual-circularly polarized wide-axial-ratio-beamwidth slot patch antenna with six-port feeding network," *IEEE Antennas and Wireless Propagation Letters*, Vol. 20, No. 12, 2486–2490, 2021.

[23] Kalfa, M. and E. Halavut, "A fast method for obtaining active S-parameters in large uniform phased array antennas," in *2013 IEEE International Symposium on Phased Array Systems and Technology*, 684–688, Waltham, MA, USA, 2013.

[24] Pozar, D. M., "The active element pattern," *IEEE Transactions on Antennas and Propagation*, Vol. 42, No. 8, 1176–1178, 1994.